

We are IntechOpen, the world's leading publisher of Open Access books Built by scientists, for scientists

6,900

Open access books available

186,000

International authors and editors

200M

Downloads

Our authors are among the

154

Countries delivered to

TOP 1%

most cited scientists

12.2%

Contributors from top 500 universities



WEB OF SCIENCE™

Selection of our books indexed in the Book Citation Index
in Web of Science™ Core Collection (BKCI)

Interested in publishing with us?
Contact book.department@intechopen.com

Numbers displayed above are based on latest data collected.
For more information visit www.intechopen.com



Chapter

Effect of Combination of Natural Dyes and the Blocking Layer on the Performance of DSSC

*Md. Mosharraf Hossain Bhuiyan, Fahmid Kabir,
Md. Serajum Manir, Md. Saifur Rahaman,
Md. Robiul Hossain, Prosenjit Barua, Bikram Ghosh,
Fumiaki Mitsugi, Tomoaki Ikegami, Saiful Huque and
Mubarak Ahmad Khan*

Abstract

Over the years, researchers have been working on replacing sensitized dye for dye sensitized solar cells (DSSC), because of its low production cost, biodegradability, and non-toxicity. However, the overall performance of natural dye-based DSSCs is low compared to the DSSCs sensitized with Ruthenium based dyes. The combination of natural dyes with an optimized choice of the extracting solvents and the proper volume ratio of mixture of the dyes, enhances inherent properties, such as absorption and adsorption of the dyes. It also allows the device to utilize photon energy more efficiently over the entire visible wavelength. As a result, DSSC sensitized with the dye mixture shows higher absorbance, and cumulative absorption properties over the whole visible region than the DSSC fabricated with individual dyes and showed higher photocurrent. Another effective way to improve cell efficiency is by using a blocking layer. The blocking layer increases the photocurrent, is mainly due to the improvement of the electron recombination at the transparent conducting oxide/electrolyte interfaces. Also, the blocking layer's compact structure creates an effective pathway for electron transportation; thus, the device's photocurrent increases. Additionally, a slight improvement in the open-circuit voltage and fill factor was observed, thus cell efficiency enhances significantly. By both the proper ratio of dye mixture and the blocking layer improves cell performance of DSSC and opens a new pathway for future studies.

Keywords: DSSC, natural dye, natural dye based DSSC, dye combination, blocking layer

1. Introduction

The global energy demand has been continuously increasing due to the continuous growth of the world population, economic development, standard of living, and drive of modern technologies. In the current situation, about 87% of the primary energy needs are mostly supplied through fossil fuels (coal, oil, and gas) [1, 2].

However, the sources of these fossil fuel reserves are depleting very fast. The existing sources of energy are inadequate, and if the fuel consumption continued at current usage rates, it would last only about 50 years [3]. On the other hand, burning fossil fuels releases carbon dioxide and other greenhouse gases (e.g., water vapor, methane, nitrous oxide, sulfur dioxide, and other ozone-depleting substance) in the atmosphere, making them the primary contributors to global warming and climate change. Because of the depletion of fossil fuels and global warming, in recent years, researchers are endeavoring severe attempts to find out various ways to meet energy demand around the world. Renewable energy could be an eco-friendly, alternative, sustainable energy resource because they are inexhaustible and will not pollute the environment for us or those of future generations by emitting harmful gases. Many alternative renewable energy sources have already been available, such as solar, hydro, wind, biogas, biomass, geothermal, wave, and tidal energy. Among all renewable resources, solar energy can be the solution to the problem of dwindling fossil-fuel reserves [4].

Solar energy is the cleanest and most abundant renewable energy source available. The solar cell or photovoltaic (PV) device is used for converting the energy of sunlight into useable electrical energy. The generated energy from solar does not produce any harmful emissions, consumes no fossil fuels, has no moving parts, and requires little maintenance. The development of PV technology is growing, and intensive research works are undertaken worldwide to improve cell performance and reduce the cost of the cell. With a history dating back over 60 years, since the very first silicon bipolar solar cell, the last three decades silicon solar cell has seen immeasurable advancement in both the performance of experimental and commercial cells. First-generation silicon solar cells showed their value in the market with the advantages, including high efficiency (26.6%), high reliability, low cost, ease of fabrication, and environmentally friendly traits [5–8]. Second generation thin-film (e.g., amorphous silicon (a-Si), cadmium telluride (CdTe), and copper indium gallium selenide (CIGS)) solar cells are cheaper than the mature Si solar cells; additionally, thin-films are easier to handle and more flexible. However, the shortage of Tellurium and Indium makes it hard to manufacture solar cells commercially. Also, Cadmium is extremely poisonous and medical problems with environmental impact [9]. This significant concern opened the method of exploration of finding other elective materials and further innovation for solar cells. Several new thinner-films have surfaced through concentrated research with higher potential, including dye-sensitized solar cell (DSSC), perovskite solar cell (PSC), copper zinc tin sulfide (CZTS) solar cell, organic solar cell (OSC), and quantum dot solar cell (QDSC) [10].

The DSSC belongs to the group of thin-films, functions on a semiconductor generated into an electrolyte and a light-sensitive anode [11]. In 1988, Brian O'Regan and Michael Grätzel at UC Berkeley, USA initially co-invented the modern version of DSSC and later they further developed this work at the École Polytechnique Fédérale de Lausanne, Switzerland [12]. Brian O'Regan and Michael Grätzel reported the first modern version of DSSC in 1991 with an efficiency of 7.1–7.9% [13, 14]. DSSC can convert the solar energy to electrical energy by using photosensitive dye. DSSC is fabricated by using conventional roll-printing systems. The semi-transparency and semi-flexibility of DSSC offer a diversity of usages not appropriate for glass-based construction and most of the materials used are low-cost. However, practical elimination of several expensive elements has proven to be difficult, notably Pt and ruthenium (Ru). The energy conversion efficiency of the most recent laboratory-developed module is approximately 14.7% [15]. This chapter is focused on the improvement of efficiency of DSSC by the combination of natural dyes and the blocking layer. In this work, structure and operation principle of the third generation dye-sensitized solar cell (DSSC) has been discussed in the second section. Section 3 explains the combination of natural dyes with an optimized

choice of the extracting solvents and the dye mixture's at proper volume ratio, enhancing the dye sensitizer's inherent properties, such as absorption and adsorption, thus improving the cell efficiency. Section 4 explains the comprehensive study of the blocking layer and its effect on the cell efficiency, and finally in section five, overall conclusions and accomplishments of this study have been mentioned.

2. Basics of DSSC

As shown in **Figure 1**, a typical DSSC consists of five different parts, such as, (1) transparent conducting oxide (TCO), glass substrate, (2) anode (wide band-gap semiconductor material layer on TCO), (3) photosensitizer, (4) electrolyte and (5) cathode (platinum/carbon layer on TCO). The components of a DSSC are: two transparent conductive oxide [indium tin oxide (ITO), fluorine-doped tin oxide (FTO), Indium Zinc Oxide (IZO) and Aluminum Zinc Oxide (AZO)] glass electrodes. One of the electrodes is the anode, the working anode, which is printed with semiconductor material [TiO_2 , ZnO , SnO_2 , SrTiO_3 , Zn_2SnO_4 , Nb_2O_5 , etc.] nanoparticles (particle size around 20–50 nm). The semiconductor oxides are sensitized with a photosensitizer (metal complex sensitizer, metal-free organic sensitizer or natural dye sensitizer), which absorbs the photons. The other electrode is the counter electrode [platinum or carbon coated TCO] and in between the two working electrodes is the electrolyte containing the redox couple [I^-/I_3^- , $\text{Br}^-/\text{Br}_3^-$, $\text{SCN}^-/(\text{SCN})_3^-$ and $\text{SeCN}^-/(\text{SeCN})_3^-$, etc.].

Figure 2 illustrates the schematic diagram of the basic working principle of a typical TiO_2 based DSSC. All other semiconductor-based DSSC such as ZnO , SnO_2 , etc. works under the same principle. Under illumination, a photo-excited electron is injected from the excited state of the dye (D^*) from the highest occupied molecule orbital (HOMO) to lowest un-occupied molecular orbital (LUMO) (Eq. (1)). The excited electron is injected to the conduction band of the semiconductor material. The injected electron percolates through the semiconductor material by a driving chemical diffusion gradient and is collected at the TCO glass substrate (Eq. (2)). After passing through an external circuit, and reaches the counter electrode, thus,

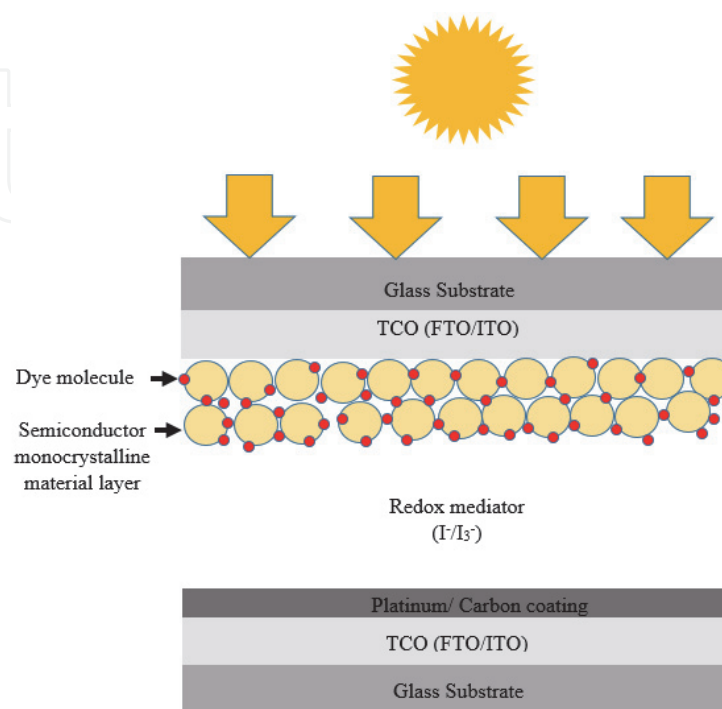


Figure 1.
Schematic diagram of basic structure of DSSC.

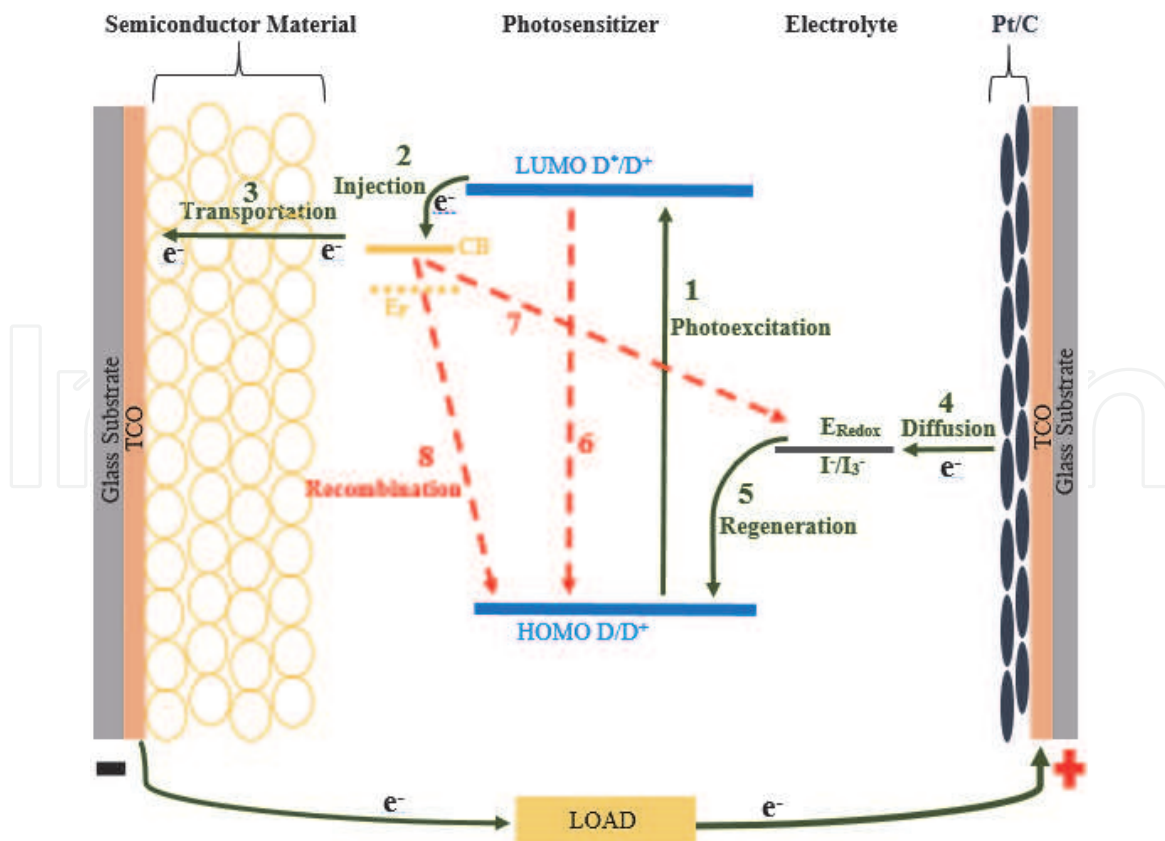
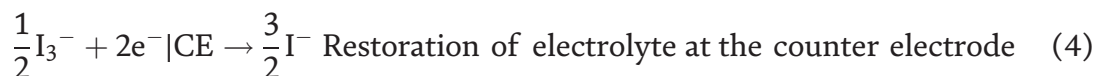
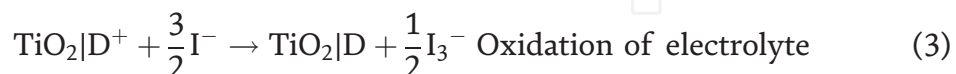
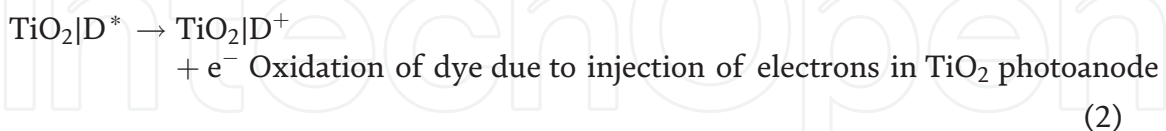
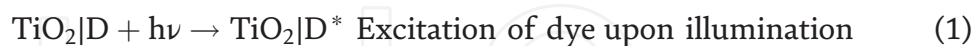


Figure 2.
Operation principal of typical DSSC.

dye regeneration takes place due to the acceptance of electrons from I^- ion redox mediator, and I^- gets oxidized to I_3^- (Eq. (3)). To complete the circle, by electron donation, I^- ions regenerated by the reduction of I_3^- ions at the cathode (Eq. (4)). However, some undesirable reactions are simultaneously taking place, such as non-radiation relaxation (Eqs. (5) and (6) no. red arrow in **Figure 2**), recombination of injected electrons with the oxidized dye (Eqs. (6) and (7) no. red arrow in **Figure 2**) and recombination of injected electrons with I_3^- (Eqs. (7) and (8) no. red arrow in **Figure 2**). In brief, the sequence of events in a DSSC is as follows [16]:



D: Dye sensitizer; D^* : Excited dye upon illumination; D^+ : Oxidized dye.

Nemours researchers are working on to improve cell performance by different means, such as modifying the TCO/semiconductor material interface by blocking layer; modifying semiconductor material by doping, annealing time, radiation,

carbon nanotubes, etc.; modifying the absorption properties of the dyes by Ru dye, organic dye, dye mixture, etc. to enhance cell efficiency [17–22].

3. Effect of combination of natural dyes

The dye in DSSCs has a vital role in harnessing solar energy from the sun and converts it into useable electrical energy. The primary charges in the dyes separate through photo-excitation, and photo-excited dyes inject electrons into the conduction band of semiconductor material. A dye should fulfill some pre-requisites to be considered efficient dye: (1) binding firmly with the semiconductor material; (2) higher molar absorption capabilities for maximum absorption from visible to IR-region; (3) fast electron transfer; (4) LUMO of the dye should be higher than the conduction band of semiconductor for efficient electron injection into the semiconductor material; (5) HOMO of the dye should be lower than the redox couple for efficient regeneration of oxidized dye; and (6) slow degradation (or do not degrade at all) [16, 23–25]. The dyes used in DSSC are divided into three types: metal complexes dye sensitizer, metal-free organic dye sensitizer, and natural dye sensitizer. Metal complexes dye sensitizers, such as polypyridyl complexes of Ruthenium (Ru), Osmium (Os), metal porphyrin, phthalocyanine are the most efficient and durable dye for DSSC application. However, these dyes have a complex synthesis process, release chemicals as a by-product, and require rare-earth material for the synthesis process. As a result, the overall fabrication process highly depended on the rare earth material that is neither sustainable nor economical. On the other hand, metal-free organic dye sensitizer has advantages over metal complex dye sensitizer, reducing the use of rare-earth material, higher molar absorption coefficient, and preprocessing color. However, these advantages are offset by their instability, tedious manufacturing process, tendency to undergo degradation, and toxicity. These significant limitations influenced scientists to work on possible replacements for metal complexes or metal-free organic dye sensitizers [16].

Over the years, significant research has been done to determine the possibility of replacing sensitized dye. Natural dye has several advantages over sensitized dyes. These include low production cost, high availability, easy access, simple fabrication technique, biodegradable, environment friendly, purity grade, non-toxic, and reducing the use of rare-earth material. Natural dye-based DSSCs have attracted considerable attraction as an alternative way to produce low-cost dyes to a large extent by extracting dyes from natural resources. In nature, some vegetables, fruits, flowers, leaves, seeds, roots, stems, bacteria, and algae exhibit various colors due to plant pigmentation [16]. The natural dyes are four major families which are chlorophyll, anthocyanin, carotenoids, and flavonoids [26, 27].

Chlorophyll, which is the most widespread pigment occurring naturally in plants, fungi, bryophytes and algae. The molecular structure of a chlorophyll consists of a Magnesium-containing tetrapyrrolic ring, encircled by other side chains. The chlorophylls are classed mainly as chlorophyll-a, chlorophyll-b, chlorophyll-c1, chlorophyll-c2, chlorophyll-d, and chlorophyll-f. They absorb light from red, blue, and violet in the visible wavelengths with an absorption maximum of ~670 nm while reflecting green wavelengths. Chlorophyll dye molecule create an electronic coupling with the conduction band of semiconductor material through the carboxylic groups, which helps to anchor the dye molecules and transfer injected electron efficiently from the dye sensitizer to the conduction band of semiconductor material [16, 28]. **Figure 3** shows the basic molecular structure of chlorophyll and the binding chlorophyll and semiconductor material (e.g., TiO₂).

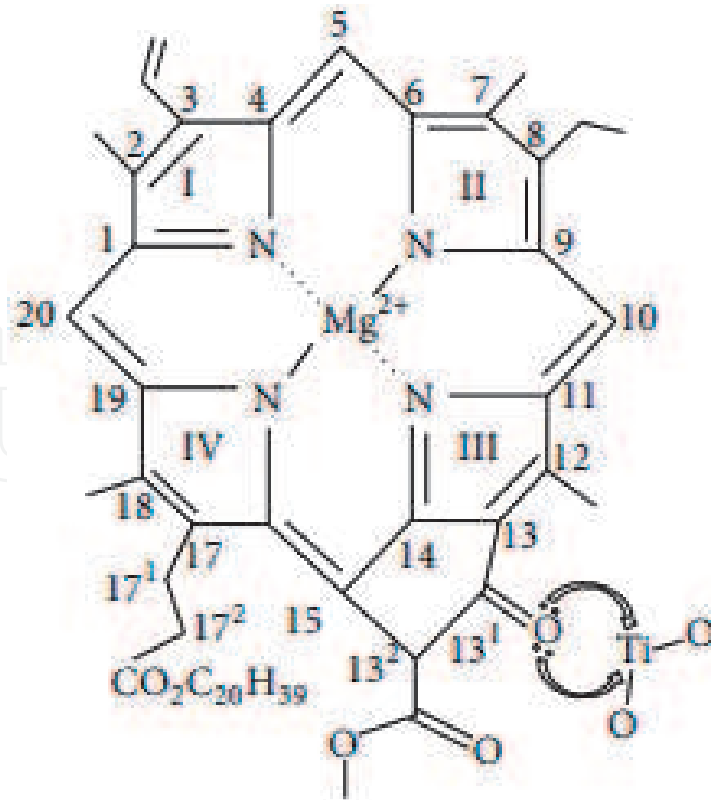


Figure 3.
Chlorophyll-semiconductor material (i.e., TiO_2) interaction [29].

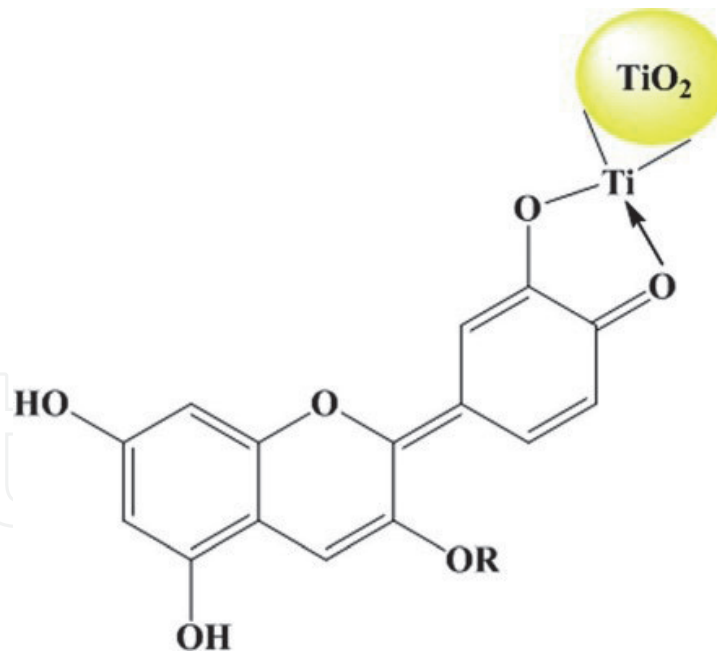


Figure 4.
Basic structure of anthocyanin and anthocyanin-semiconductor material (TiO_2) interaction [31].

Anthocyanins are also an abundant and widespread group of water-soluble pigments in plants. They absorb light at the longest wavelengths. Depending on the pH value, anthocyanins are responsible for the existence of attractive colors, such as red, orange, magenta, pink, blue, blue-black and purple floral [16, 30]. Generally, the carbonyl and hydroxyl functional groups in the anthocyanin dye sensitizers create an electronic coupling with the semiconductor material's conduction band, which helps transfer the excited electron efficiently to the conduction band of

semiconductor material [16]. **Figure 4** shows the basic interaction between anthocyanin and semiconductor material (e.g., TiO_2).

Carotenoids occur in many plants and algae, as well as several bacteria, and fungi. It contributes to yellow, orange, and red colors and allows them to absorb short-wave visible light [32]. Carotenoids can be divided into two major types: xanthophylls (with oxygen) and carotenes (purely hydrocarbons and without oxygen) [16, 33]. **Figure 5** illustrates the interaction between carotenoids- semiconductor material (i.e., TiO_2).

Flavonoids are essential floral pigments. The development of a specific color depends on the accumulation of flavonoid chromophores and other intrinsic and extrinsic factors. Chemically, the flavonoids have a C6- C3- C6 carbon framework with two connected two phenyl rings (A and B) and a heterocyclic ring (C). Depending on the oxidation potential of the C-ring, the particular flavonoids absorb light in the visible wavelength. Till now, over 5000 flavonoids have been identified from different plants. Most of the flavonoid pigment has loosely or unbound electrons. Thus less energy is required for excitation of such electrons is lower compared to the others. As a result, those pigment molecules can be energized by the light within the visible range [16].

The overall cell efficiency of natural dye-based DSSCs is comparably low compared to DSSCs sensitized with sensitized dyes. Due to the inadequate interaction between dyes and semiconductor surface, a significant reduction of the cell's short-circuit current. The pigment's long structure obstructs the dye molecules to form a bond with the oxide surface of the semiconductor materials effectively. Those are the field of works that are yet to be developed in natural dye DSSCs to achieve high-efficiency devices and device stability. To further raise the efficiency of the DSSC combination of dyes has been explored and reported DSSC or to broaden the absorption spectrum [35–39]. A combination of natural dyes with an optimized choice of the extracting solvent enhances the absorption of solar light and allowed utilization of the photon energy more efficiently. As a result, DSSC sensitized with the dye mixture shows higher absorbance, and cumulative absorption properties over the entire visible region than the DSSC fabricated with single individual dyes [35, 36].

Kabir et al. studied the effect of chlorophyll and anthocyanin dye mixture on the cell performance of natural dye-based DSSC. They also mixed the dyes at five different volume ratios to find the optimized dye mixture. The cell conversion efficiency of DSSC fabricated with individual chlorophyll, and anthocyanin dyes

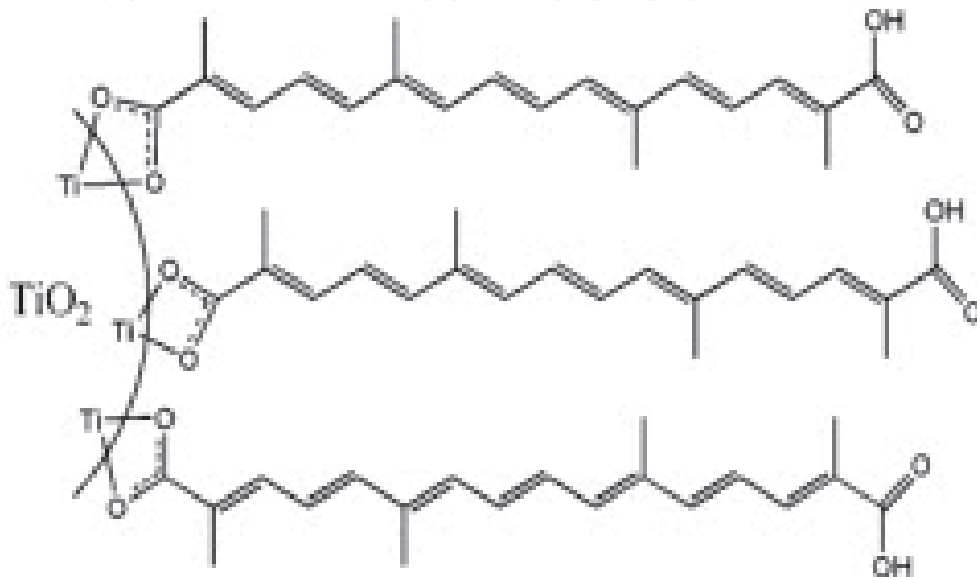


Figure 5.
Carotenoids -semiconductor material (i.e., TiO_2) interaction [34].

were 0.466% and 0.531%, respectively. DSSC co-sensitized with the optimized dye mixture (20% chlorophyll + 80% anthocyanin) showed cell conversion efficiency of 0.847%, which is almost 1.82 and 1.6 times higher than the cell efficiency of the individual chlorophyll and anthocyanin dye-sensitized DSSC's (shown in **Figure 6**). The chemical characteristics study of the dye showed that no new bond except has formed; however, few shifts in the adsorption peak was observed (Shown in **Figure 7** and **Table 1**). Similar characteristics were seen when dyes were adsorbed the TiO_2 semiconductor material (shown in **Figure 8**. and **Table 2**, [36].

Figure 9 illustrates the UV-visible absorption spectra of natural chlorophyll (green), anthocyanin (red), and the optimum combination of dyes (green + red) diluted in ethanol. The dye mixture has demonstrated the cumulative absorption properties of both individual green and red dye.

Kabir et al. also studied the effect of betalain and curcumin dye combination on the cell performance of natural dye-based DSSC. They also mixed the dyes at three different volume ratios to find the optimized dye combination. The optimized dye mixture demonstrated the cumulative absorption properties of both individual betalain and curcumin dye (shown in **Figure 10**). The DSSC fabricate with the combination of betalain and curcumin dye also showed superior cell performance than DSSC manufactured with individual betalain and curcumin dye (shown in **Figure 11** and **Table 3**) [35].

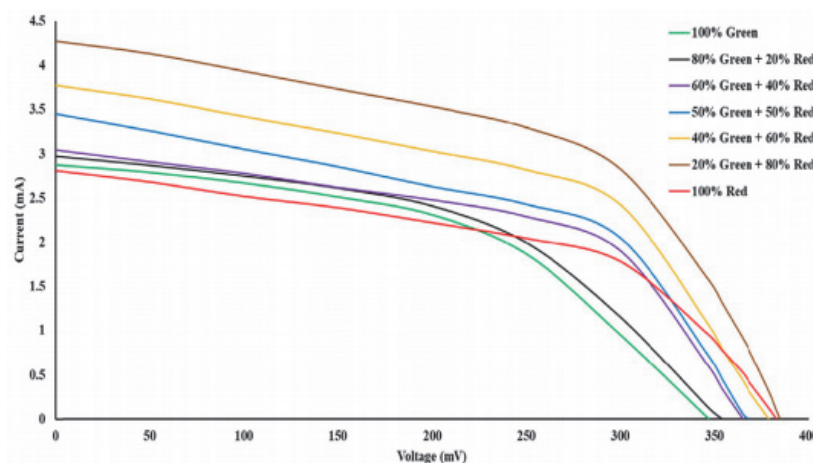


Figure 6. I-V characteristics of DSSC fabricated with chlorophyll, anthocyanin and different combinations [36].

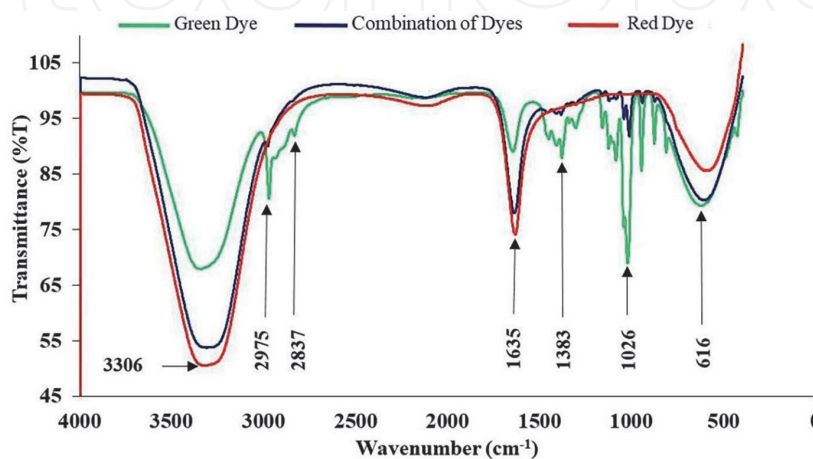


Figure 7. FT-IR adsorption spectra of natural chlorophyll (green), anthocyanin (red), and combination (20% green + 80% red) of dyes (without TiO_2) [36].

Functional group	Absorption range (in cm^{-1})	Type of vibration	Intensity	Absorption peak of green dye (in cm^{-1})	Absorption peak of combination of dyes (in cm^{-1})	Absorption peak of red dye (in cm^{-1})
Alkyl Halide (C—Cl)	600–800	Stretch	Strong	616	610	606
Alkene (=C—H)	675–1000	Bending	Strong	944	950	—
Ether (C—O)	1000–1300	Stretch	Strong	1017	1026	—
Amine (C—N)	1080–1360	Stretch	Weak	1338	1354	—
Aromatic (C=C)	1400–1600	Stretch	Medium weak	1422	1404	—
Alkene (C=C)	1620–1680	Stretch	Variable	1652	1619	1635
Alkane (C—H)	2820–2850	Stretch (symmetric)	Strong	2837	—	—
Alkane (C—H)	2850–3000	Stretch (asymmetric)	Strong	2975	—	—
Alcohol (O—H)	3200–3600	Stretch	Broad and strong	3346	3320	3329

Table 1. IR absorption of organic functional groups of natural green, red, and combination of dyes (20% green + 80% red) without TiO_2 [36].

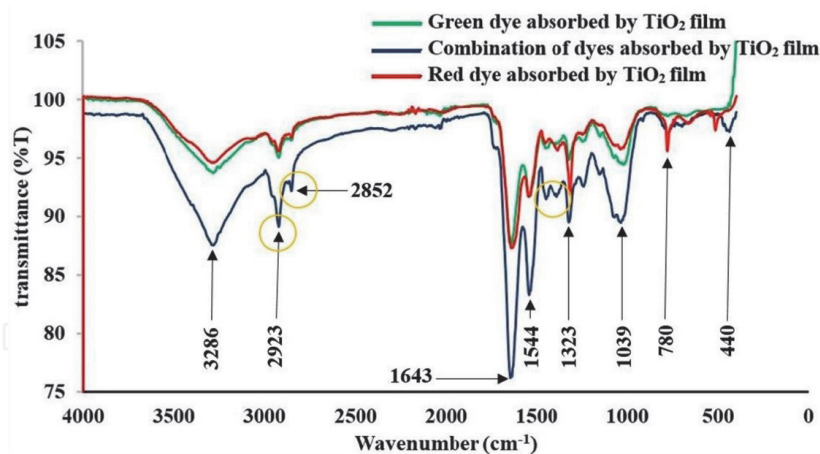


Figure 8. FT-IR adsorption spectra of natural chlorophyll (green), anthocyanin (red), and combination (20% green + 80% red) of dyes (with TiO_2) [36].

Nonetheless, to the best of our knowledge, combination of dyes have a positive impact on the cell performance of natural based DSSC.

4. Effect of blocking layer in DSSC

In DSSCs, a porous layer of nanostructured semiconductor materials such as TiO_2 [40–45], ZnO [46–48], SnO_2 [49, 50], SrTiO_3 [51, 52] Zn_2SnO_4 [53, 54] and Nb_2O_5 [55] called a photo anode, covered with photosynthetic dye. The photo anode of

Functional group	Absorption range (in cm^{-1})	Type of vibration	Intensity	Absorption peak of green dye by TiO_2 film (in cm^{-1})	Absorption peak of combination of dyes by TiO_2 film (in cm^{-1})	Absorption peak of red dye by TiO_2 film (in cm^{-1})
Ti—O—Ti	400–800	Stretch	Strong	438	440	515
Alkene (=C—H)	675–1000	Bending	Strong	817	782	780
Ether (C—O)	1000–1300	Stretch	Strong	1042	1039	1040
Amine (C—N)	1080–1360	Stretch	Weak	1324	1323	1315
Aromatic (C=C)	1400–1600	Stretch	Medium weak	1546	1544	1538
Alkene (C=C)	1620–1680	Stretch	Variable	1639	1643	1636
Alkane (C—H)	2820–2850	Stretch (symmetric)	Strong	2848	2852	2856
Alkane (C—H)	2850–3000	Stretch (asymmetric)	Strong	2924	2923	2924
Alcohol (O—H)	3200–3600	Stretch	Broad and strong	3384	3286	3281

Table 2.

IR absorption of organic functional groups of natural green, red, and combination of dyes (20% green + 80% red) with TiO_2 [36].

DSSC influences the photo generated current. Highly porous structures and large surface areas of the nanostructured semiconductor materials increase the dye absorption and move the photo-induced electron towards the load [56]. Intensive research has been undertaken by the DSSC research community to increase photo-induced current and understand the mechanisms responsible for losses in the cell. Radiation less relaxation of energized dye, electron recombination with the oxidized dye; and electron recombination with the tri-iodide in the electrolyte are the main reasons for limiting the photocurrent in the cell. Generally, the first two have a negligible impact, while the last one shows a significant impact [56, 57].

Electron recombination occurs when electron transfer to I_3^- in the electrolytes via semiconductor material and the TCO. Electron recombination through both routes needs to be reduced to prevent loss. In I^-/I_3^- redox couple, the electron transfer via the TCO is negligible due to small exchange current density between I_3^-/I^- . Generally, the losses via the FTO under short-circuit condition is insignificant, because the Fermi level of the TCO (i.e., FTO) is close to the redox Fermi level. However, under illumination, the quasi-Fermi level of the semiconductor material (i.e., TiO_2) rises rapidly with distance from the TCO (as shown in **Figure 12a**). As a result, a higher driving force is observed when electron transfer from the semiconductor material to I_3^- , which is much higher than in the bulk of the sensitized layer that is close to the TCO glass substrate. Thus, I_3^- electrons are anticipated to recombine with the semiconductor material at short-circuit conditions [57].

However, under illumination, the open-circuit condition is entirely different (shown in **Figure 12b**). Due to the rise (~ 0.7 eV) of the Fermi level of TCO glass substrate, a much higher driving force is observed when electron transfer from the TCO glass substrate to I_3^- . Thus, the electron recombination with I_3^- via the TCO glass substrate and the back reaction by these two routes causes a photo stationary state in the cell [57].

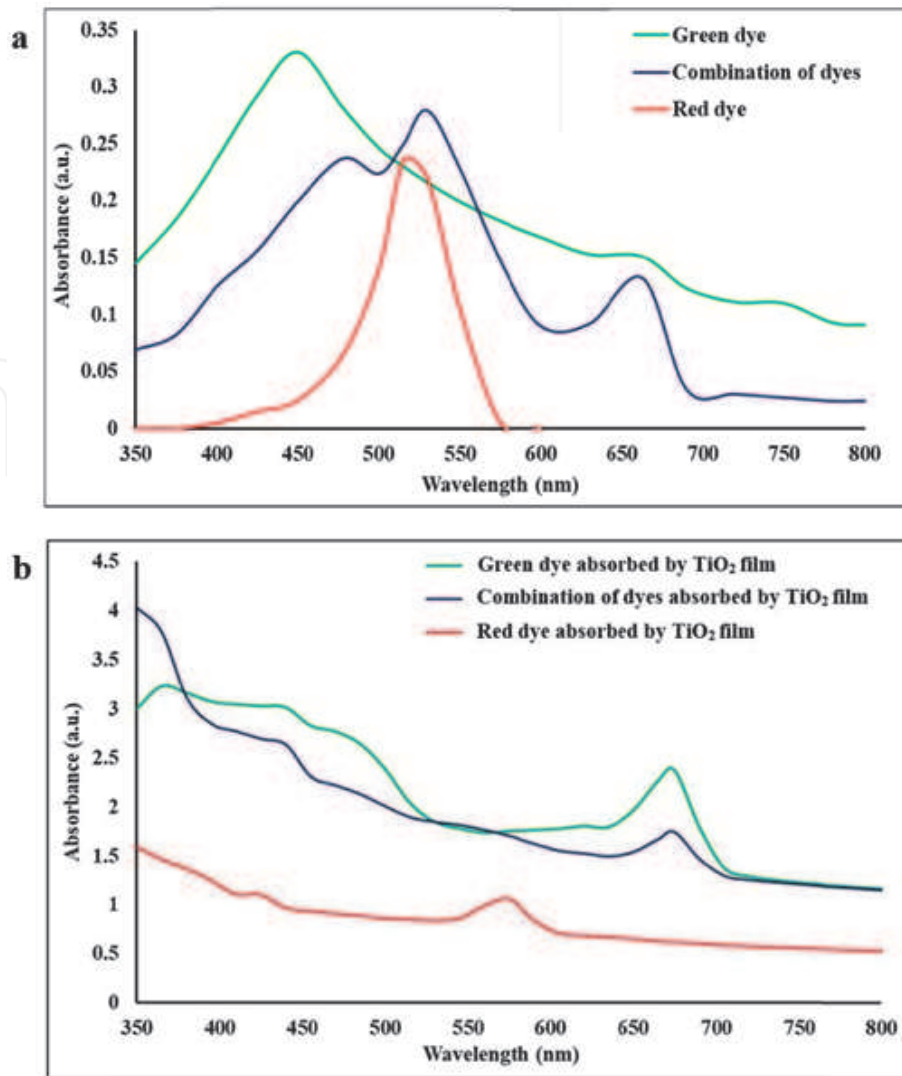


Figure 9.
 (a) Absorption spectra of diluted natural chlorophyll (green), anthocyanin (red), and the optimum combination of dyes without TiO₂, and (b) absorption spectra of diluted natural chlorophyll (green), anthocyanin (red), and the optimum combination of dyes with TiO₂ [36].

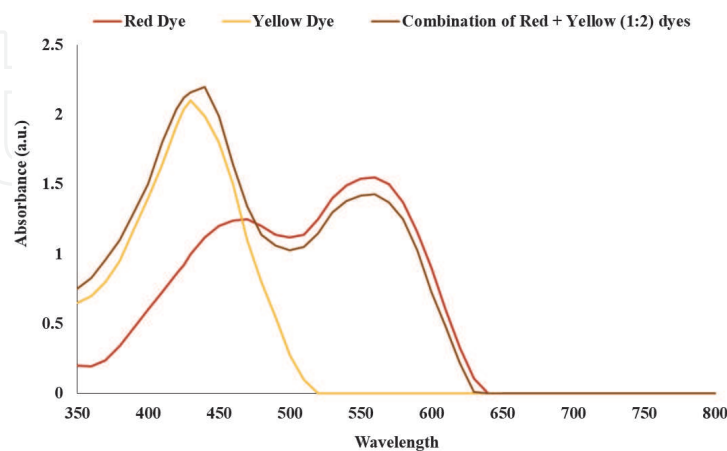


Figure 10.
 Absorption properties of betalain, curcumin, and combination of dyes [35].

The blocking layer works as a barrier layer at the TCO/semiconductor material interface to improve cell performance. Studies had shown that a significant improvement in photo induced current observed when the blocking layer was introduced in the cell. Park and colleagues found that due to the blocking layer's

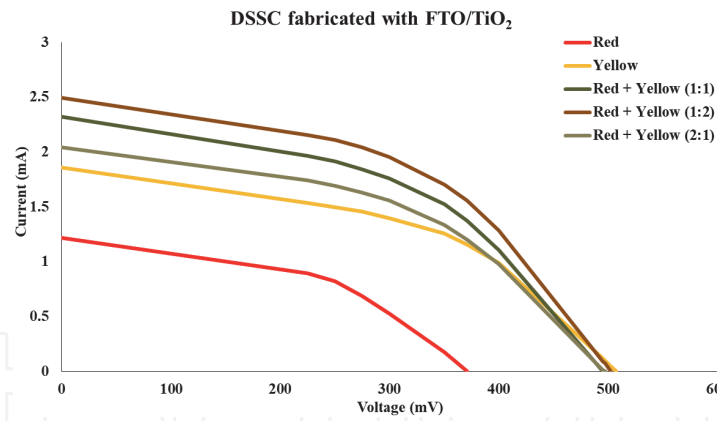


Figure 11. I-V characteristics of DSSC fabricated with betalain, curcumin, and combination of dyes [35].

Dye/ Combination of dyes	Dye ratio	V_{oc} (mV)	I_{sc} (mA)	FF	$\eta\%$	Dye loading (mol mm^{-3} $\times 10^7$)
Red		371.6 ± 09.5	1.218 ± 0.039	0.487 ± 0.008	0.220 ± 0.016	1.05
Yellow		507.2 ± 10.5	1.857 ± 0.026	0.503 ± 0.004	0.473 ± 0.020	1.09
Red + Yellow	1:1	495.5 ± 09.4	2.319 ± 0.015	0.508 ± 0.003	0.583 ± 0.018	1.09
Red + Yellow	1:2	502.7 ± 11.5	2.494 ± 0.022	0.518 ± 0.002	0.649 ± 0.020	1.08
Red + Yellow	2:1	497.1 ± 14.3	2.041 ± 0.025	0.508 ± 0.003	0.515 ± 0.024	1.09

Table 3. Photovoltaic performance of DSSC fabricated with FTO/TiO₂ [35].

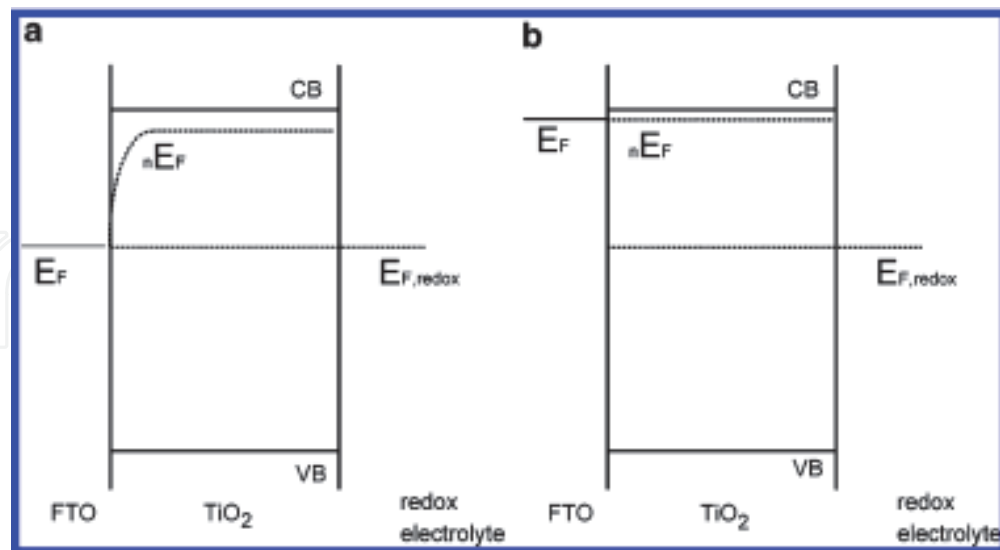


Figure 12. Schematic of DSSC in the absence of a blocking layer. (a) under short circuit conditions, the Fermi level in the FTO is close to the redox Fermi level results in rapid electron-transfer kinetics to I₃⁻. (b) under open-circuit conditions, the Fermi level in the FTO moves up as the electron quasi-Fermi level rises and results in a photo stationary state [57].

presence, total transfer resistance at the blocking layer/electrolyte interface increased that increased cell performances by preventing electron recombination near the TCO glass substrate [58, 59]. Fabregat and co-workers found that BL

improved physical contact between the TCO and semiconductor material that produce higher photo conversion efficiency. However, the advantage obtained by utilizing blocking layer is lost if the layer is too thick, and, generally, generates a series of resistance and an electron barrier that reduces the charge collection efficiency [59, 60].

A significant amount of photo-induced electron recombined and results in lower photocurrent. Recombination of the electron at the interfaces reduces the photocurrent and affects the fill factor; thus, cell performance decreases [60]. The complete photo anode is constructed layer-by-layer stack of suitably designed structures to maximize different cell functionalities. The recombination losses in DSSCs occurred primarily at the interface between the glass substrate of TCO and the electrolyte. The compact blocking layer acts as a physical barrier and physically separates and reduces the contact surface area between the TCO glass substrate from the electrolyte [59]. By employing the blocking layer with suitable thickness, the recombination can be reduced; and photo induced current and fill factor increase, leading to the DSSC efficiency improvement. Studies also showed that the blocking layer also improved the open-circuit-photo voltage of the cell [61]. The schematic on the effect of blocking layer is shown in **Figure 13**.

There are many kinds of preparation methods for blocking layers in DSSCs, including spin coating, deep coating, spray coating, sol-gel, sputtering, hydrothermal technique, etc. Spin-coating is a simple method for preparing uniform thin films onto flat substrates. Generally, the spin coating method includes deposition, spinup, spinoff, and evaporation [62]. Usually, a small amount of coating material is applied to the center of the substrate then rotated at speed up to 10,000 rpm to spread the coating material by centrifugal force. Rotation is continued while the fluid spins off the substrate's edges until the desired thickness of the film is

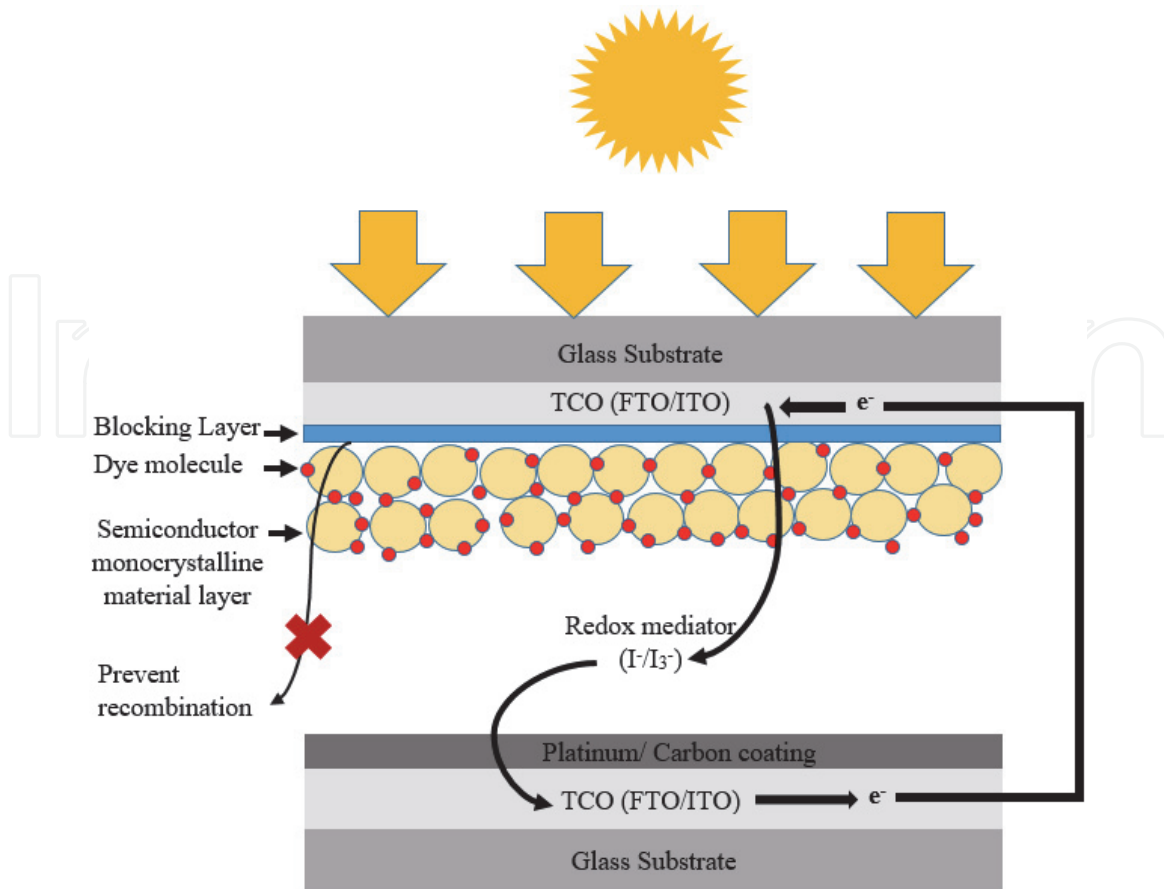


Figure 13.
Schematic diagram of the DSSC including a blocking layer for preventing recombination.

achieved. The film's thickness also depends on the solvent and solvents concentration [63].

Yeol et al. prepared a ZnO precursor on FTO substrates for the blocking layer. For ZnO precursor, a homogeneous mixture of 2.195 g zinc acetate dehydrate, 20 mL isopropanol, and 0.605 mL monoethanolamine (MEA) was prepared. The concentration was 0.5 M, with MEA: zinc acetate molar ratio of 1: 1. The prepared solution was stirred for 2 hrs at 200 rpm at 60°C, then stirred at the same rpm at ambient temperature for 22 hrs. For the spin-coated film, rotation speed and duration were held at 3000 rpm and 20 s, respectively. They annealed the spin-coated films at 500° C for 1 h to form a blocking layer of ZnO (55 nm to 310 nm). The ZnO blocking layer thickness is a function of the number of deposition cycles in the spin-coating process. ZnO blocking layer thickness increased linearly with the number of deposition cycles, a typical feature of the spin-coating technique [64]. **Figure 14a** illustrates the morphology of FTO. **Figure 14b** and **c** show that ZnO nanoparticles are distributed uniformly across the FTO substrate's surface to form a compact layer. Comparing both **Figure 14a** and **c**, when the thickness of the ZnO blocking layer increased, the size of the ZnO nanoparticles also slightly increased.

Yeol et al. showed that the effect of ZnO blocking layer and increasing its thickness on the cell performance of TiO₂ based DSSC. **Table 4** lists photovoltaic performance and **Figure 15** illustrates the J–V characteristics of the cell, including ZnO blocking layers of different thicknesses. The value of open-circuit voltage (V_{oc}) and fill factor (FF) of the DSSC improves, though the short-circuit current decreased. The increase of open-circuit voltage is due to the blocking of electron injection from the TiO₂ conduction band to the FTO [64, 65]. Due to the increased electron density in the TiO₂, the Fermi level rises. However, further an increase in the thickness of the ZnO blocking layer, the value of short circuit current decreased

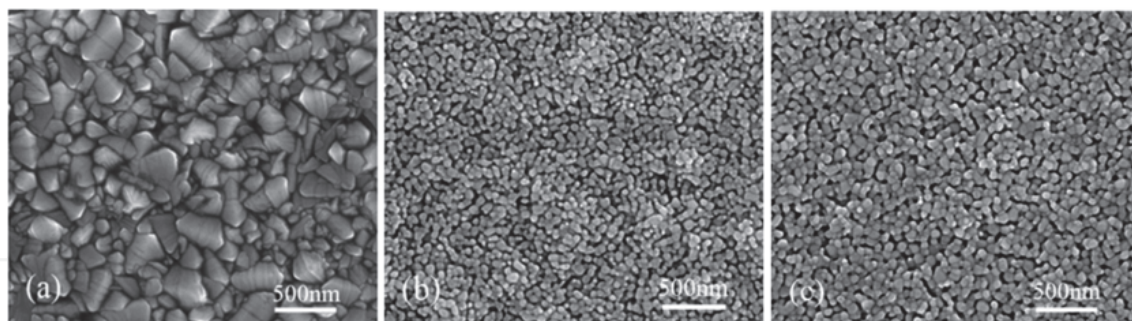


Figure 14. FESEM images of (a) bare FTO, (b) FTO/ ZnO blocking layer (120 nm), (c) FTO/ ZnO blocking layer (310 nm) [64].

Sample	V_{oc} (mV)	J_{sc} (mA/cm ²)	Efficiency (% η)	Fill Factor (FF)
FTO	695	8.48	3.86	0.66
FTO/ZnO (55 nm)	708	8.30	3.96	0.67
FTO/ZnO (120 nm)	728	8.18	4.34	0.73
FTO/ZnO (220 nm)	744	6.64	3.63	0.73
FTO/ZnO (275 nm)	745	4.83	2.69	0.75
FTO/ZnO (310 nm)	781	3.05	1.66	0.70

Table 4. Photovoltaic properties of TiO₂ based DSSCs including ZnO blocking layer of different thicknesses (for N3 dye) [64].

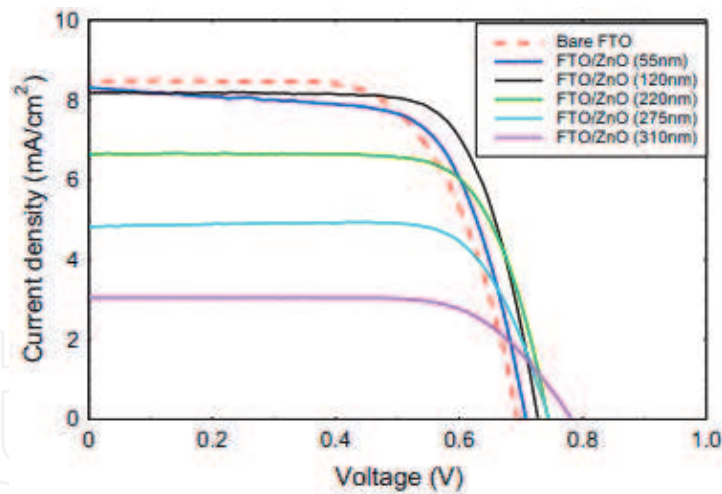


Figure 15.
J–V characteristics of DSSCs including ZnO blocking layer of different thicknesses [64].

Revolution per minute (rpm)	Thickness (nm)	Rughness (nm)
0	0	21.14
2000	10–30	10.91
1000	40–60	11.68
500	120–150	14.05

Table 5.
Thickness and root-mean-square roughness of TiO₂ thin films [66].

rapidly. As a result, cell performance decrease despite the slight improvement in the V_{oc} and FF values because the excessively thick ZnO layer blocks the electron injection from the conduction band of TiO₂ to the FTO substrate [64].

Lee et al. introduced an additional spin-coated TiO₂ thin film between the FTO and TiO₂ (semiconductor material) as a blocking layer for the electron injected from the exited photosensitizer. A homogeneous mixture of 29.0 mg titanium tetraisopropoxide [Ti (OC₃H₇)₄], and 100 ml isopropanol [(CH₃)₂CHOH] was prepared. Then the solution of 7.5 ml HCl in 100 ml of isopropanol was added drop by drop to the [Ti (OC₃H₇)₄]-[(CH₃)₂CHOH] solution at 0°C under continuous stirring, and afterward the solution was allowed to stand for less than 1 h at the same temperature. The solution was smeared on FTO substrates and rotated at 500, 1000, and 2000 rpm for 40 s to ensure uniformity. The samples were heated for 1 h at 100°C; they were sintered for 30 min at 450°C [66].

Lee et al. prepared several TiO₂ gel films with the spin coating method with different thicknesses. The thickness and roughness of the TiO₂ layers are among the most critical factors in the cell performance of DSSC [66]. **Table 5** lists the thickness and root-mean-square roughness of TiO₂ thin films. SEM images of 10 μm thin films (surface and cross-sections) are shown in **Figure 16**. **Table 6** lists photovoltaic performance and **Figure 17** illustrates the J–V characteristics of the cell, including ZnO blocking layers of different thicknesses.

TiO₂ layers also enhance the contact property between the FTO and TiO₂ electrode. **Figure 16c** and **d** illustrate the photovoltaic performance and the J–V characteristics curve of DSSC with different blocking layer thicknesses. The thickness of the TiO₂ blocking layer affects the efficiency of DSSC. As thin films' rpm increased, the thickness and roughness of the TiO₂ blocking layer also decreased, and the film becomes smooth and uniform. This increase in the smoothness and uniformity of

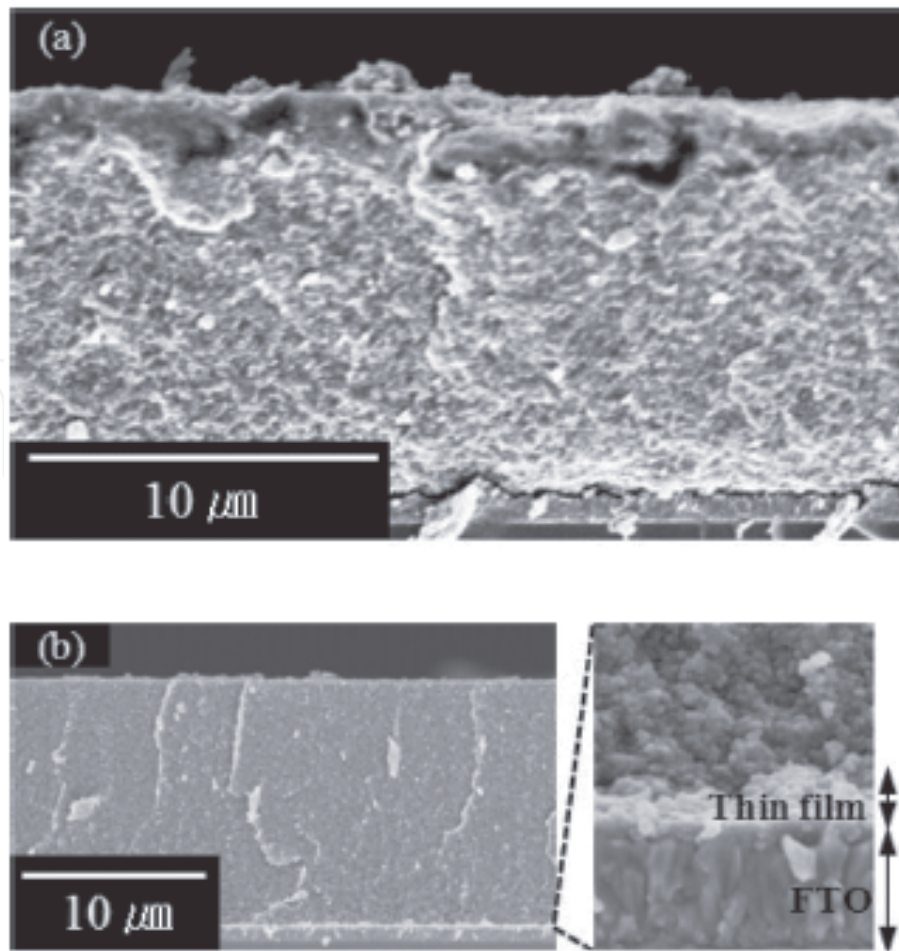


Figure 16. Cross-sectional SEM images of the main-TiO₂/FTO (a), main-TiO₂/TiO₂ thin film/FTO applied to a DSSC (b) [66].

Thickness (nm)	Open-circuit voltage, V _{oc} (V)	Short-circuit current density, J _{sc} (mA/cm ²)	Fill factor, FF (%)	Efficiency, η (%)	Electron lifetime, T _e (ms)	Resistance at Pt. counter electrode, R _{Ct1} (Ω)	Charge transfer resistances at the TiO ₂ /dye/electrolyte interface R _{Ct2} (Ω)
0	0.65	11.09	62	4.43	14.1	5.3	28.8
10–30	0.74	11.92	64	5.62	20.1	4.3	19.1
40–60	0.72	11.58	65	5.39	18.2	4.7	19.7
120–150	0.70	11.21	60	4.68	16.6	7.6	21.9

Table 6. The cell performance of DSSCs based on TiO₂ layers (10.5 μm) compressed at different thickness of thin films during the preparation for ruthenium 535 (Solaronix Co. N3) dye [66].

the TiO₂ blocking layer results in improved cell performance. The increased number of efficiently transferred photo generated electrons to the TiO₂ electrode results in an improvement in short-circuit current [67]. By suppressing the recombination of electrons injected from excited photosensitizers in the TiO₂ and electrolyte interface, a higher value of open-circuit voltage was obtained [57]. Their study also showed that when the resistance at the FTO/TiO₂ layer interface was decreased, the electron lifetime in DSSCs was increased [66].

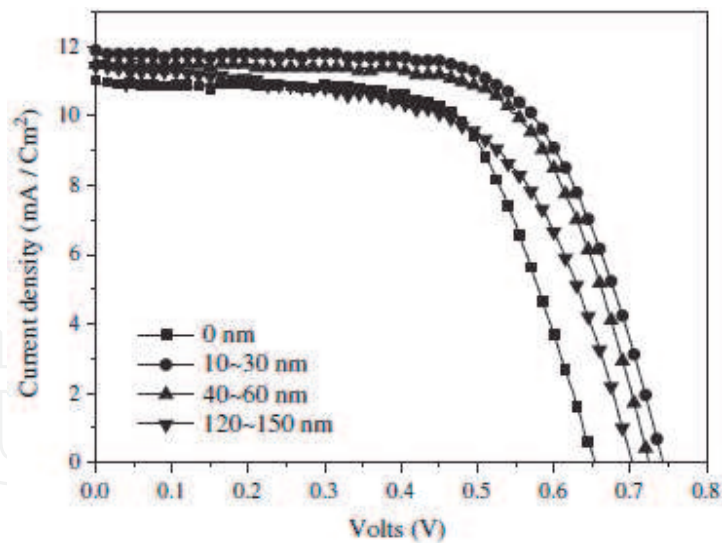


Figure 17.
I-V curves for DSSCs with TiO_2 blocking layers at different thickness [66].

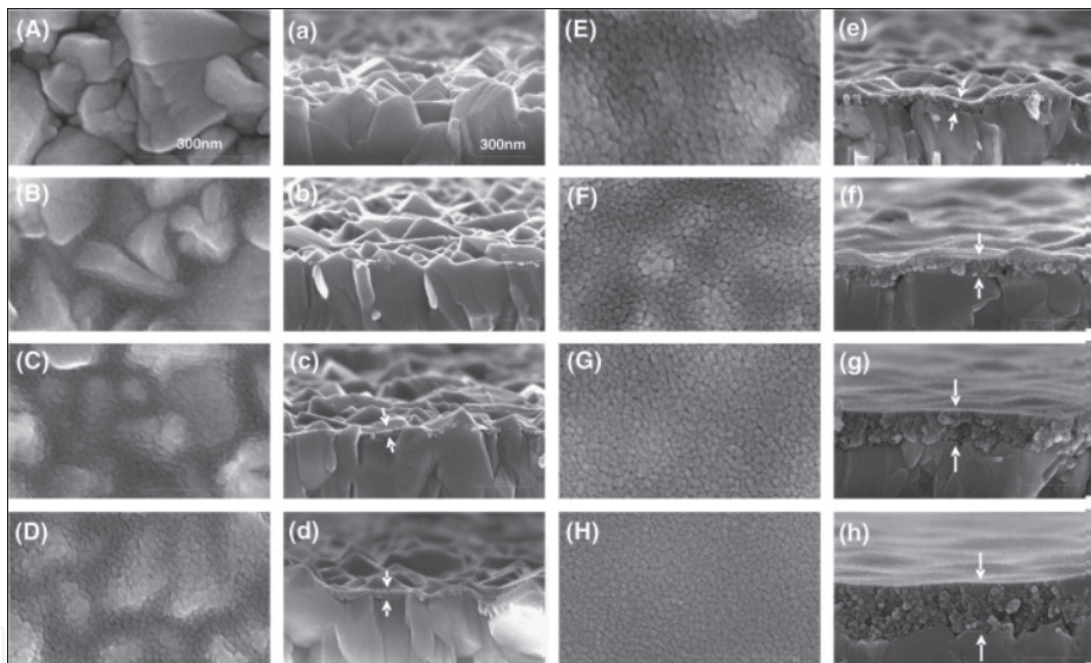


Figure 18.
Surface (A–H) and cross-section (a–h) SEM micrographs for the bare FTO, blocking layer-deposited FTO substrates from the Ti precursor solutions with the concentration of 0.05, 0.1, 0.15, 0.2, 0.4, 0.8, and 1.2 M, respectively [58].

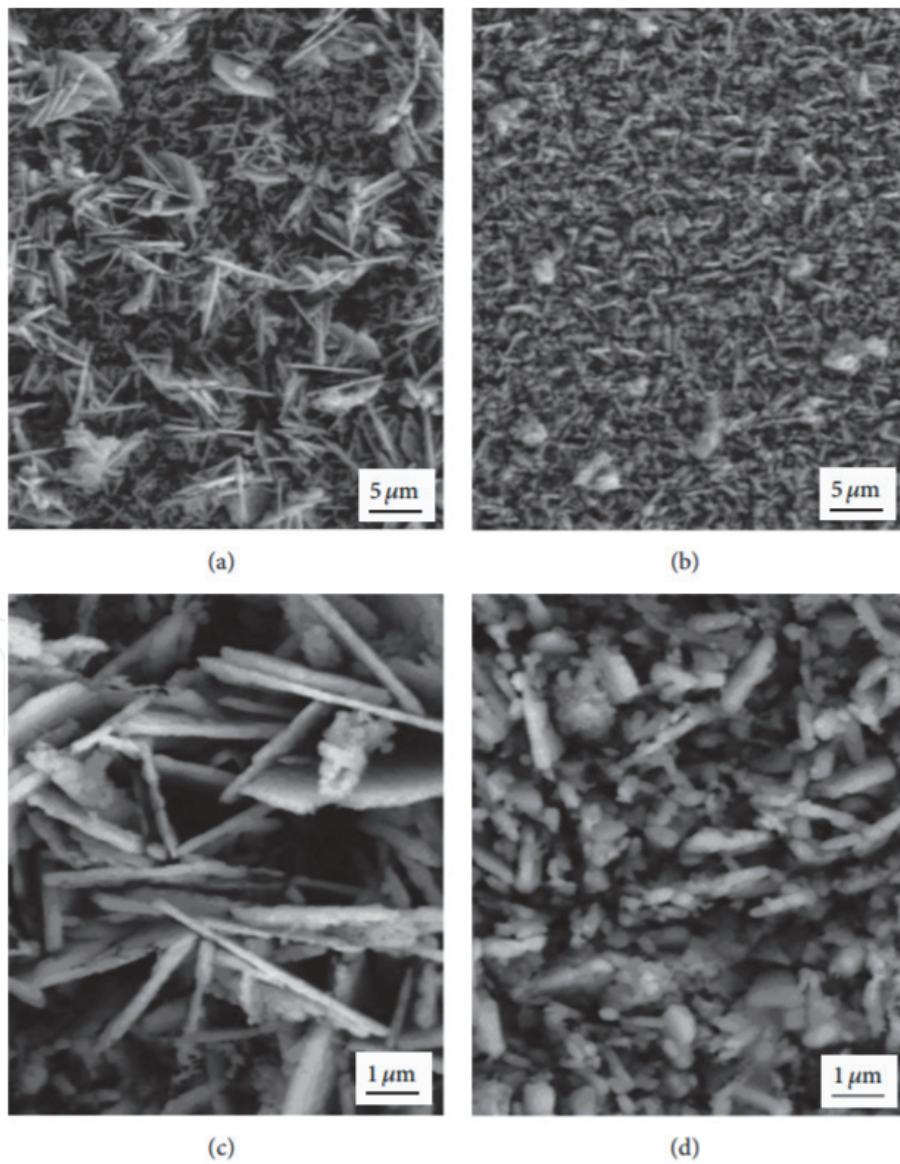
Yoo et al. showed the impact of precursor concentration in the cell conversation efficiency of DSSC. For the blocking layer, a 1-butanol solution contained titanium (IV) bis(ethylacetoacetato) di-isopropoxide precursor was spin-coated on an FTO glass, followed by annealing at 500°C in air for 30 min. The concentration of the solution was varied from 0.05 M to 1.2 M [58]. **Figure 18** illustrates the SEM of bare FTO and blocking layer-deposited FTO glasses (surface and cross-sections). **Table 7** lists the photovoltaic property of DSSC with a blocking layer, where short-circuit current density increases with increasing the precursor concentration (and increased blocking layer thickness).

Zou et al. studied the effect of the TiCl_4 blocking layer (or pre-treatment) in ZnO based DSSC. **Figure 19** shows the fabricated ZnO films, with and without TiCl_4 pre-treatment on the FTO glass substrate. From **Figure 19a-d**, it can be seen that fabricated ZnO films have porous flakes, both with and without blocking

Ti precursor concentration (M)	Short-circuit current, J_{sc} (mA/cm ²)	Open-circuit voltage, V_{oc} (V)	Fill factor, FF	Efficiency, η (%)	Area (cm ²)
Without blocking layer	0.01	0.588	0.356	0.002	0.99
0.05	0.05	0.861	0.475	0.020	0.99
0.10	0.08	0.865	0.482	0.033	1.02
0.15	0.10	0.869	0.530	0.046	1.02
0.20	0.14	0.871	0.564	0.069	1.02
0.40	0.21	0.881	0.618	0.114	1.02
0.80	0.38	0.884	0.648	0.218	1.02
1.20	0.56	0.883	0.615	0.304	1.02

Table 7.

Photocurrent-voltage characteristics of DSSC comprising only blocking layers for N719 dye [58].

**Figure 19.**

SEM images of (a) FTO/ZnO with $TiCl_4$ pretreatment, (b) FTO/ZnO without $TiCl_4$ pretreatment, (c) and (d) the amplification figure of (a) and (b), respectively [68].

Samples	Open-circuit voltage, V_{oc} (V)	Short-circuit current, J_{sc} (mA/cm ²)	Fill factor, FF	Efficiency, η (%)
Without TiCl ₄	0.3977	1.07	0.2829	0.12
TiCl ₄	0.4759	2.86	0.3967	0.54

Table 8.
 Photovoltaic performance of ZnO based DSSCs with TiCl₄ pretreatment and without TiCl₄ pretreatment [68].

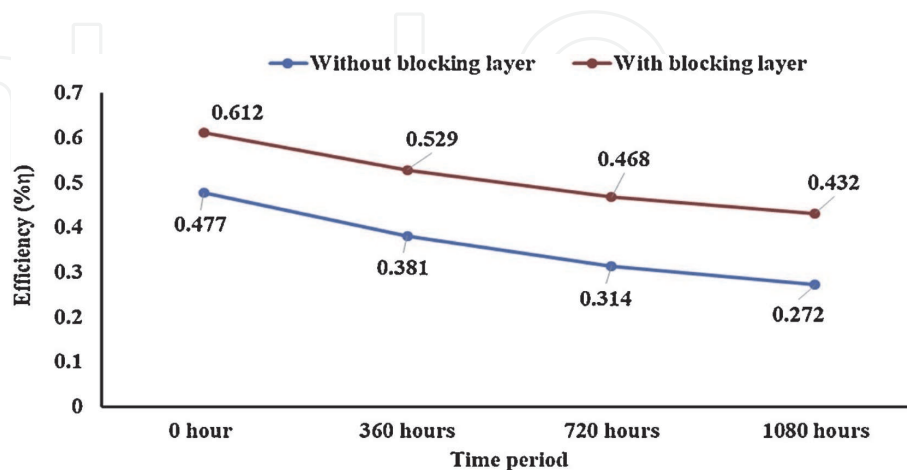


Figure 20.
 Effect of post TiCl₄ treatment in the cell performance of TiO₂ based DSSC [69].

layers. However, TiCl₄ treated ZnO anode has a larger flake, which can offer a large surface area to absorb much more dyes. **Table 8** lists the photovoltaic property of DSSC with TiCl₄ blocking layer [68].

Kabir et al. studied the effect of post-treatment of TiCl₄ in TiO₂ based DSSC. Post TiCl₄ treatment not only increases the overall cell conversion efficiency of DSSC but also enhances cell stability. TiCl₄ treated TiO₂ anode based DSSC's degradation rate is much lower than the TiCl₄ untreated TiO₂ anode based DSSC. Studies showed that TiCl₄ treated TiO₂ anode based DSSC's cell stability of the increase around 38–44.5%. **Figure 20** shows the effect of post TiCl₄ treatment in the cell conversion efficiency of TiO₂ based DSSC [69].

Cameron et al. [57], Heo et al. [70], Yu et al. [71] used spray coating method to prepare TiO₂ blocking layer. Introducing the blocking layer into the device decreases charge carrier trapping and recombination. Subsequently, short-circuit current increases significantly. Additionally, a slight improvement in the open-circuit voltage and fill factor is observed, thus cell efficiency enhances significantly.

5. Summary

In conclusion, natural dye is a promising alternative to replace the metal complexes or organic dyes in the DSSC application. They are low-cost, abundant, eco-friendly, simple extraction procedures, and non-toxic. The combination of natural dyes with an optimized choice of the mixture of the volume ratio of the extracting dye extracting solvent accounts for many possible interactions that promise to provide more charge injection upon sensitization and allowed utilization of the photon energy more efficiently. DSSC co-sensitized with the dye mixture shows higher absorbance, and cumulative absorption properties over the entire visible region than the DSSC fabricated with individual dyes.

A blocking layer in DSSC provides good adhesion between the transparent conducting oxide (e.g., ITO, FTO, etc.) and an active semiconductor layer, TCO (e.g., TiO₂, ZnO, etc.). It also represses the electron back transport between electrolyte and TCO by blocking direct contact. Also, it offers a more uniform layer than bare TCO glass substrate. The conventional blocking suppresses electron leakage, recombination, and trapping; thus, the photovoltaic performance of the DSSC improves. Introducing a blocking layer in the DSSCs show lower dark current and operates efficiently under high-intensity sunlight and ambient light conditions.

Acknowledgements

This work is supported by the by the Ministry of Science & Technology, Government of the People's Republic of Bangladesh under the Special Allocation Research project for Science & Technology, FY 2019-2020, entitled, "Development of nanotechnology based solar cells using low cost natural dyes extracted from vegetables and the effect of gamma radiation on its performance", (Ref. No.: 39.00.0000.009.06.024.19/ID-478-494).

Author details

Md. Mosharraf Hossain Bhuiyan^{1,2*}, Fahmid Kabir³, Md. Serajum Manir⁴, Md. Saifur Rahaman¹, Md. Robiul Hossain³, Prosenjit Barua³, Bikram Ghosh³, Fumiaki Mitsugi⁵, Tomoaki Ikegami⁵, Saiful Huque³ and Mubarak Ahmad Khan⁴

1 Institute of Nuclear Science and Technology, Atomic Energy Research Establishment, Bangladesh Atomic Energy Commission, Dhaka, Bangladesh

2 Department of Computer Science and Engineering, Central University of Science and Technology, Mirpur, Dhaka, Bangladesh

3 Institute of Energy, University of Dhaka, Dhaka, Bangladesh

4 Institute of Radiation and Polymer Technology, Atomic Energy Research Establishment, Bangladesh Atomic Energy Commission, Dhaka, Bangladesh

5 Faculty of Advanced Science and Technology, Kumamoto University, Kumamoto, Japan

*Address all correspondence to: mosharraf22003@yahoo.com; mosharraf22003@baec.gov.bd

IntechOpen

© 2021 The Author(s). Licensee IntechOpen. This chapter is distributed under the terms of the Creative Commons Attribution License (<http://creativecommons.org/licenses/by/3.0>), which permits unrestricted use, distribution, and reproduction in any medium, provided the original work is properly cited. 

References

- [1] "OPEC: Organization of the Petroleum Exporting Countries, 2011. World Oil Outlook," [Online]. Available: http://www.opec.org/opec_web/static_files_project/media/downloads/publications/WOO_2011.pdf.
- [2] "OPEC: Organization of the Petroleum Exporting Countries, 2012. World Oil Outlook," [Online]. Available: http://www.opec.org/opec_web/static_files_project/media/downloads/publications/WOO2012.pdf.
- [3] R. R. Baadhe, R. Potumarthi and V. Gupta, "Lipase-Catalyzed Biodiesel Production: Technical Challenges," Elsevier, 2014, pp. 119–129.
- [4] N. Thejo Kalyani and S. J. Dhoble, "Empowering the Future With Organic Solar Cell Devices," *Nanomaterials for Green Energy*, 2018, p. 325–350.
- [5] J. Liu, Y. Yao, S. Xiao and X. and Gu, "Review of status developments of high-efficiency crystalline silicon solar cells," *Journal of Physics D: Applied Physics*, vol. 51, no. 12, p. 123001., 2018.
- [6] T. D. Lee and A. and U. Ebong, "A review of thin film solar cell technologies and challenges," *Renewable and Sustainable Energy Reviews*, vol. 70, pp. 1286–1297, 2017.
- [7] F. Kabir and e. al., "Stability study of natural green dye based DSSC," *Optik*, vol. 181, pp. 458–464, 2019.
- [8] M. M. H. Bhuiyan and e. al., "Economic evaluation of a stand-alone residential photovoltaic power system in Bangladesh," *Renewable Energy*, vol. 21, no. 3–4, pp. 403–410, 2000.
- [9] V. Fthenakis and K. and Zweibel, "Fthenakis, V. and Zweibel, K., 2003. CdTe PV: Real and perceived EHS risks (No. NREL/CP-520-33561)," in *National Renewable Energy Lab. (NREL)*, Golden, CO (United States)., 2003.
- [10] "Third-generation photovoltaic cell," [Online]. Available: https://en.wikipedia.org/wiki/Third-generation_photovoltaic_cell. [Accessed 20 7 2020].
- [11] M. Fitra, I. Daut, N. Gomesh, M. Irwanto and Y. and M. Irwan, "Dye solar cell using Syzigium Oleina organic dye," *Energy Procedia*, Vols. 341–348., pp. 341–348., 2013.
- [12] "Dye-sensitized solar cell," [Online]. Available: https://en.wikipedia.org/wiki/Dye-sensitized_solar_cell. [Accessed 20 07 2020].
- [13] B. O'Regan and M. and Grätzel, "A Low-Cost, High-Efficiency Solar Cell Based on Dye-Sensitized Colloidal TiO₂ Films," *Nature*, vol. 353, pp. 737–740, , 1991 .
- [14] M. Grätzel, "Dye-sensitized solar cells," *Journal of Photochemistry and Photobiology C: Photochemistry Reviews*, vol. 4, p. 145–153. , 2003.
- [15] K. Kakiage, Y. Aoyama, T. Yano, K. Oya, J. I. Fujisawa and M. and Hanaya, "Highly-efficient dye-sensitized solar cells with collaborative sensitization by silyl-anchor and carboxy-anchor dyes," *Chemical Communications*, vol. 51, no. 88, pp. 15894–15897, 2015.
- [16] N. T.R.N. Kumara and e. al., "Recent progress and utilization of natural pigments in dye sensitized solar cells: A review," *Renewable and Sustainable Energy Reviews*, vol. 78, pp. 301–317, 2017.
- [17] K. Balachandran and e. al., "Enhancing power conversion efficiency of DSSC by doping SiO₂ in TiO₂ photo anodes," *Materials Science in Semiconductor Processing*, vol. 35, pp. 59–65, 2015.

- [18] B. Roose and e. al., "Doping of TiO₂ for sensitized solar cells," *Chemical Society Reviews*, vol. 44, no. 22, pp. 8326–8349, 2015.
- [19] F. Kabir and e. al., "Effect of MWCNT's concentration in TiO₂ based DSSC and degradation study of the cell," *Journal of Renewable and Sustainable Energy*, vol. 11, no. 2, p. 023502, 2019.
- [20] A. Islam and e. al., "Enhanced photovoltaic performances of dye-sensitized solar cells by co-sensitization of benzothiadiazole and squaraine-based dyes," *ACS applied materials & interfaces*, vol. 8, no. 7, pp. 4616–4623, 2016.
- [21] T. A. Ruhane and e. al., "Photo current enhancement of natural dye sensitized solar cell by optimizing dye extraction and its loading period," *Optik*, vol. 149, pp. 174–183, 2017.
- [22] T. A. Ruhane and e. al., "Impact of photo electrode thickness and annealing temperature on natural dye sensitized solar cell," *Sustainable energy technologies and assessments*, vol. 20, pp. 72–77, 2017.
- [23] G. Calogero and e. al., "Synthetic analogues of anthocyanins as sensitizers for dye-sensitized solar cells," *Photochemical & Photobiological Sciences*, vol. 12, no. 5, pp. 883–894, 2013.
- [24] A. Hagfeldt and e. al., "Dye-Sensitized Solar Cells," *Chem. Rev.*, vol. 10, no. 11, p. 6595–6663, 2010.
- [25] J. A. Mikroyannidis and e. al., "Low band gap dyes based on 2-styryl-5-phenylazo-pyrrole: Synthesis and application for efficient dye-sensitized solar cells," *Journal of Power Sources*, vol. 196, no. 8, pp. 4152–4161, 2011.
- [26] S. Shalini and e. al., "Review on natural dye sensitized solar cells: Operation, materials and methods," *Renewable and Sustainable Energy Reviews*, vol. 51, p. 1306–1325, 2015.
- [27] M. R. Narayan, "Review: Dye sensitized solar cells based on natural photosensitizers," *Renewable and Sustainable Energy Reviews*, vol. 16, no. 1, pp. 208–215, 2012.
- [28] Y. Amao and e. al., "Preparation and properties of dye-sensitized solar cell using chlorophyll derivative immobilized TiO₂ film electrode," *Journal of Photochemistry and Photobiology A: Chemistry*, vol. 164, no. 1–3, pp. 47–51, 2004.
- [29] H. C. Hassan and e. al., "A High Efficiency Chlorophyll Sensitized Solar Cell with Quasi Solid PVA Based Electrolyte," *International Journal of Photoenergy*, p. Article ID 3685210, 2016.
- [30] K. Davies, *Plant pigments and their manipulation.*, Blackwell publishing, 2004.
- [31] I. C. Maurya and e. al., "Natural dye extracted from saraca asoca flowers as sensitizer for TiO₂-based dye-sensitized solar cell," *Journal of Solar Energy Engineering*, vol. 138, no. 5, 2016.
- [32] C. Zho and e. al., "The regulation of carotenoid pigmentation in flowers," *Archives of Biochemistry and Biophysics*, vol. 504, no. 1, pp. 132–141, 2010.
- [33] E. Murillo, "Native carotenoids composition of some tropical fruits," *Food Chemistry*, vol. 140, no. 4, pp. 825–836, 2013.
- [34] E. C. Prima, "Performance of natural carotenoids from *Musa aromatica* and *Citrus medica* var Lemon as photosensitizers for dye-sensitized solar cells with TiO₂ nanoparticle," *Advanced Materials Research*, vol. 789, pp. 167–170, 2013.
- [35] F. Kabir and e. al., "Enhance cell performance of DSSC by dye mixture, carbon nanotube and post TiCl₄ treatment along with degradation study," *Sustainable Energy Technologies*

and Assessments, vol. 35, pp. 298–307, 2019.

[36] F. Kabir and e. al., "Development of dye-sensitized solar cell based on combination of natural dyes extracted from Malabar spinach and red spinach," *Results in Physics*, vol. 14, p. 102474, 2019.

[37] F. Kabir and e. al., "Effect of combination of natural dyes and post-TiCl₄ treatment in improving the photovoltaic performance of dye-sensitized solar cells," *Comptes Rendus Chimie*, vol. 22, no. 9–10, pp. 659–666, 2019.

[38] D. D. Pratiwi and e. al., "Performance improvement of dye-sensitized solar cells (DSSC) by using dyes mixture from chlorophyll and anthocyanin," *Journal of Physics: Conference Series*, vol. 909, p. 012025, 2017.

[39] H. Bashar and e. al., "Study on combination of natural red and green dyes to improve the power conversion efficiency of dye sensitized solar cells," *Optik*, vol. 185, pp. 620–625, 2019.

[40] F. Kabir, M. M. H. Bhuiyan, M. R. Hossain, H. Bashar, M. S. Rahaman, M. S. Manir, S. M. Ullah, S. S. Uddin, M. Z. I. Mollah, R. A. Khan and S. and Huque, "Improvement of efficiency of Dye Sensitized Solar Cells by optimizing the combination ratio of Natural Red and Yellow Dyes," *Optik*, vol. 179, pp. 252–258, 2019.

[41] k. Usha, B. Mondal, D. Sengupta and e. al., "Development of multilayered nanocrystalline TiO₂ thin films for photovoltaic application," *Optical Materials*, vol. 36, no. 6, pp. 1070–1075, 2014.

[42] W. Q. Wu, Y. F. Xu, C. Y. Su and D. B. Kuang, "Ultra-long anatase TiO₂ nanowire arrays with multi-layered configuration on FTO glass for high-efficiency dye-sensitized solar

cells," *Energy & Environmental Science*, vol. 7, no. 2, pp. 644–649, 2014.

[43] P. Sun, X. Zhang, L. Wang, F. Li, Y. Wei, C. Wang and Y. and Liu, "Bilayer TiO₂ photoanode consisting of a nanowire–nanoparticle bottom layer and a spherical voids scattering layer for dye-sensitized solar cells," *New Journal of Chemistry*, vol. 39, no. 6, pp. 4845–4851, 2015.

[44] H. H.G. Tsai, C. J. Tan and W. and H. Tseng, "Electron transfer of squaraine-derived dyes adsorbed on TiO₂ clusters in dye-sensitized solar cells: a density functional theory investigation," *The Journal of Physical Chemistry C*, vol. 119, no. 9, pp. 4431–4443, 2015.

[45] A. K.Chandiran, F. Sauvage, M. Casas-Cabanas, P. Comte, S. M. Zakeeruddin and M. Graetzel, "Doping a TiO₂ photoanode with Nb⁵⁺ to enhance transparency and charge collection efficiency in dye-sensitized solar cells," *The Journal of Physical Chemistry C*, vol. 114, no. 37, pp. 15849–15856, 2010.

[46] D. Sengupta, P. Das, U. Kasinadhuni, B. Mondal and K. Mukherjee, "Morphology induced light scattering by zinc oxide polydisperse particles: promising for dye sensitized solar cell application," *Journal of Renewable and Sustainable Energy*, vol. 6, no. 6, p. 063114, 2014.

[47] X. Chen, Z. Bai, X. Yan, H. Yuan, G. Zhang, P. Lin, Z. Zhang, Y. Liu and Y. Zhang, "Design of efficient dye-sensitized solar cells with patterned ZnO–ZnS core–shell nanowire array photoanodes," *Nanoscale*, vol. 6, no. 9, pp. 4691–4697., 2014.

[48] L. Lin, X. Peng, S. Chen, B. Zhang and Y. Feng, "Preparation of diverse flower-like ZnO nanoaggregates for dye-sensitized solar cells," *RSC Advances*, vol. 5, no. 32, pp. 25215–25221, 2015.

- [49] K. Manseki, T. Sugiura and T. Yoshida, "Microwave synthesis of size-controllable SnO₂ nanocrystals for dye-sensitized solar cells," *New Journal of Chemistry*, vol. 38, no. 2, pp. 598–603, 2014.
- [50] H. J. Snaith and C. Ducati, "SnO₂-based dye-sensitized hybrid solar cells exhibiting near unity absorbed photon-to-electron conversion efficiency," *Nano letters*, vol. 10, no. 4, pp. 1259–1265, 2010.
- [51] E. Guo and L. Yin, "Tailored SrTiO₃/TiO₂ heterostructures for dye-sensitized solar cells with enhanced photoelectric conversion performance," *Journal of Materials Chemistry A*, vol. 3, no. 25, pp. 13390–13401, 2015.
- [52] C. W. Kim, S. P. Suh, M. J. Choi, Y. S. Kang and Y. S. Kang, "Fabrication of SrTiO₃-TiO₂ heterojunction photoanode with enlarged pore diameter for dye-sensitized solar cells," *Journal of Materials Chemistry A*, vol. 1, no. 38, pp. 11820–11827, 2013.
- [53] Y. F. Wang, K. N. Li, Y. F. Xu, H. S. Rao, C. Y. Su and D. B. Kuang, "Hydrothermal fabrication of hierarchically macroporous Zn₂SnO₄ for highly efficient dye-sensitized solar cells," *Nanoscale*, vol. 5, no. 13, pp. 5940–5948., 2013.
- [54] C. Chen, Y. Li, X. Sun, F. Xie and M. Wei, "Efficiency enhanced dye-sensitized Zn₂SnO₄ solar cells using a facile chemical-bath deposition method," *New Journal of Chemistry*, vol. 38, no. 9, pp. 4465–4470, 2014.
- [55] D. Hwang, J. S. Jin, H. Lee, H. J. Kim, H. Chung, D. Y. Kim and S. K. D. Y. Jang, "Hierarchically structured Zn₂SnO₄ nanobeads for high-efficiency dye-sensitized solar cells," *Scientific reports*, vol. 4, p. 7353, 2014.
- [56] T. S. Bramhankar and e. al., "Effect of Nickel–Zinc Co-doped TiO₂ blocking layer on performance of DSSCs," *Journal of Alloys and Compounds*, vol. 817, p. 152810, 2020.
- [57] P. J. Cameron and L. M. Peter, "Characterization of titanium dioxide blocking layers in dye-sensitized nanocrystalline solar cells," *The Journal of Physical Chemistry B*, vol. 107, no. 51, pp. 14394–14400, 2003.
- [58] B. Yoo and e. al., "Chemically Deposited Blocking Layers on Fto Substrates: Effect of Precursor Concentration on Photovoltaic Performance of Dye-Sensitized Solar Cells," *Journal of Electroanalytical Chemistry*, vol. 638, no. 1, pp. 161–166, 2010.
- [59] G. S. Selopal and e. al., "Effect of blocking layer to boost photoconversion efficiency in ZnO dye-sensitized solar cells," *ACS applied materials & interfaces*, vol. 6, no. 14, pp. 11236–11244, 2014.
- [60] M. S. Goes and e. al., "Impedance spectroscopy analysis of the effect of TiO₂ blocking layers on the efficiency of dye sensitized solar cells," *The Journal of Physical Chemistry C*, vol. 116, no. 23, pp. 12415–12421, 2012.
- [61] Z. Shaban and e. al., "Optimization of ZnO thin film through spray pyrolysis technique and its application as a blocking layer to improving dye sensitized solar cell efficiency," *Current Applied Physics*, vol. 16, no. 2, pp. 131–134, 2016.
- [62] S. Ahmadi and e. al., "The role of physical techniques on the preparation of photoanodes for dye sensitized solar cells," *International Journal of Photoenergy*, vol. Article ID 198734, 2014.
- [63] "Spin coating," [Online]. Available: https://en.wikipedia.org/wiki/Spin_coating. [Accessed 20 07 2020].
- [64] M. E. Yeoh and K. and Y. Chan, "Efficiency enhancement in

dye-sensitized solar cells with ZnO and TiO₂ blocking layers," *Journal of Electronic Materials*, vol. 48, no. 7, pp. 4342–4350., 2019.

[65] Y. Liu and e. al., "Influences on photovoltage performance by interfacial modification of FTO/mesoporous TiO₂ using ZnO and TiO₂ as the compact film," *Journal of alloys and compounds*, vol. 509, no. 37, pp. 9264–9270., 2011.

[66] J. G. Lee and e. al., "Enhancement of photovoltaic performance in dye-sensitized solar cells with the spin-coated TiO₂ blocking layer," *Journal of nanoscience and nanotechnology*, vol. 12, pp. 6026–6030, 2012.

[67] B. Pradhan and e. al., "Vertically aligned ZnO nanowire arrays in Rose Bengal-based dye-sensitized solar cells," *Solar energy materials and solar cells*, vol. 91, no. 9, pp. 769–773, 2007.

[68] X. Zou and e. al., "TiCl₄ Pretreatment and Electrodeposition Time Investigations of ZnO Photoelectrodes Preparation for Dye Sensitized Solar Cells," *International Journal of Photoenergy*, p. Article ID 890563, 2014.

[69] F. Kabir and S. N. Sakib, "Various impacts of blocking layer on the cell stability in natural dye based dye-sensitized solar cell," *Optik*, vol. 180, pp. 684–690, 2019.

[70] J. Heo and e. al., "Room temperature synthesis of highly compact TiO₂ coatings by vacuum kinetic spraying to serve as a blocking layer in polymer electrolyte-based dye-sensitized solar cells," *Journal of Thermal Spray Technology*, vol. 24, no. 3, pp. 328–337, 2015.

[71] H. Yu and e. al., "An efficient and low-cost TiO₂ compact layer for performance improvement of dye-sensitized solar cells," *Electrochimica Acta*, 54(4), pp.1319–1324., vol. 54, no. 4, pp. 1319–1324, 2009.